

**Fig. 1:** (a) S K-edge XANES of PFBT and PFBT/CN in darkness and under illumination. (b) C K-edge XANES of PFO/CN, PCzF/CN, PFBT/CN and  $g\text{-C}_3\text{N}_4$  in darkness and under illumination. (c) N K-edge XANES of PFO/CN, PCzF/CN, PFBT/CN, and  $g\text{-C}_3\text{N}_4$  in darkness and under illumination. (dot-dashed lines: in darkness; solid lines: under illumination). [Reproduced from Ref. 1]

tra of the PHJ in **Figs. 1(b) and 1(c)** are derived from the heptazine rings of  $g\text{-C}_3\text{N}_4$ . The C K-edge spectra of  $g\text{-C}_3\text{N}_4$  and PHJ upon irradiation showed greater intensity than under darkness, indicating that more empty states were created in the LUMO of  $g\text{-C}_3\text{N}_4$ . Notably, the decreased intensities of the PHJ are due to charge transfer from the LUMO of PF to the C sites in  $g\text{-C}_3\text{N}_4$ . The N K-edge spectra of both PFO/CN and PFBT/CN show enhanced intensities under illumination, whereas the N K-edge intensity of PCzF/CN decreases under illumination. This fact indicates that electron transfer from PCzF to the N sites in  $g\text{-C}_3\text{N}_4$  is more facile, which might account for the charge-transfer dynamics of PCzF/CN more accelerated than of PFO/CN and PFBT/CN. Together with the significantly increased intensity of the N K-edge in PFBT/CN under illumination, it can be deduced that there is an electron migration from the N site of the heptazine rings back to the S site in PFBT.

In summary, PHJ formed via intermolecular  $\pi\text{-}\pi$  interactions were developed for stable and efficient photocatalytic SHC. A strategy of molecular design was further proposed toward increased photocatalytic activities, through modification of the polymer molecules for efficient exciton dissociation or extended light absorption. Potentially, through rational molecular design, the band energy levels of the organic semiconductors can be further optimized to attain wide-band optical absorption as well as efficient charge separation, to achieve high photocatalytic SHC efficiency over the entire solar spectrum. (Reported by Yan-Gu Lin)

*This report features the work of Shaohua Shen and his co-workers published in Adv. Mater. 29, 1606198 (2017).*

#### TLS 20A1 BM – (H-SGM) XAS

#### TLS 16A1 BM – Tender X-ray Absorption, Diffraction

- XANES, EXAFS
- Material Science, Chemistry, Condensed Matter Physics, Environmental and Earth Science

#### Reference

1. J. Chen, C.-L. Dong, D. Zhao, Y.-C. Huang, X. Wang, L. Samad, L. Dang, M. Shearer, S. Shen, and L. Guo, *Adv. Mater.* **29**, 1606198 (2017).

## Probing the Structural Evolution of a Battery with X-rays

*Spectra and scattering have given significant insight into battery reactions.*

**B**atteries to store electric energy have attracted intense attention because of the steadily increasing demands of mobile and stationary applications. In principle, the capacity of an electrode to store charge is related to the number of ionic intercalants that is limited by their size, and is also dependent on the structure and morphol-

ogy of the electrode materials. There is a necessity to investigate electrode materials with a large ion-intercalation capacity with minimal side reactions. Further, it is important to investigate and to understand the ion-electrode intercalation reactions in relation to the electrochemical voltage plateaus, which might hold the key to future battery development. In particular, to comprehend what happens in battery materials in the charge or discharge process, we should know the variation of the local electronic state in a valence-selective manner.

Bing-Joe Hwang (National Taiwan University of Science and Technology) and his co-workers recently developed a rechargeable Al-ion battery (AIB) using a

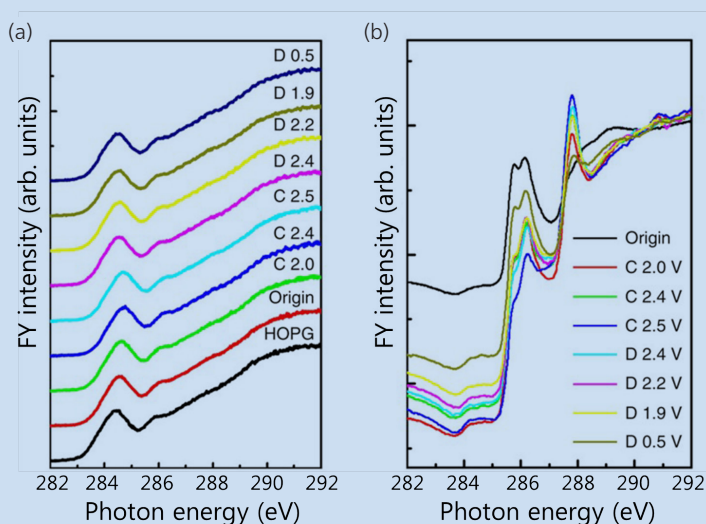


**Fig. 1:** X-ray absorption spectra of graphite at the C–K-edge. (a) Fluorescence (fluorescence yield, FY) mode and (b) total-electron-yield (TEY) modes of natural graphite in various charging and discharging states (denoted C and D, respectively) through the second cycle. HOPG: highly oriented pyrolytic graphite. [Reproduced from Ref. 1]

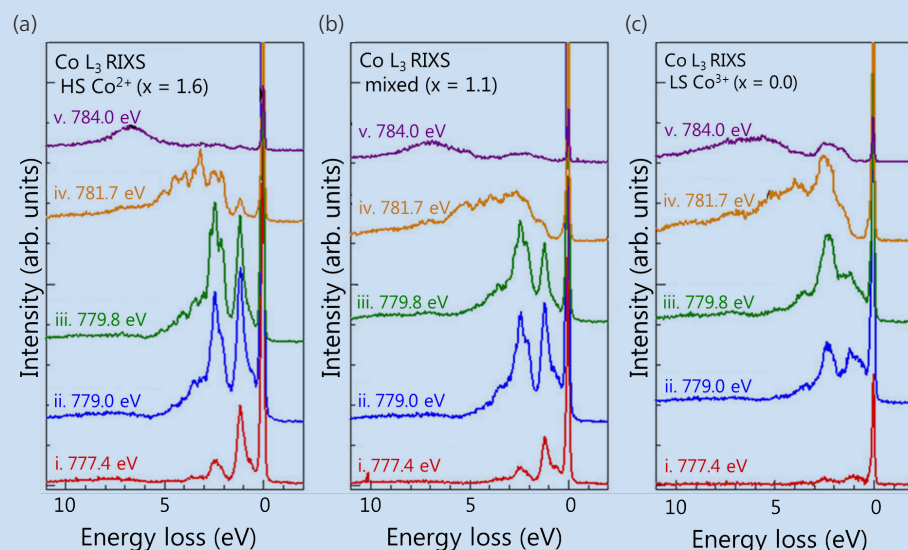


**Fig. 2:** RIXS spectra about the Co  $L_3$ -edge of  $\text{Na}_x \text{Co}[\text{Fe}(\text{CN})_6]$  films: (a)  $x = 1.6$ , (b) 1.1, and (c) 0.0; the spectra are normalized to the incident photon flux. [Reproduced from Ref. 2]

film of SP-1 natural graphite flakes (NG) with a polyvinylidene fluoride (PVDF) binder as the cathode.<sup>1</sup> Employing X-ray spectra at NSRRC beamline **TLS 20A1**, the authors studied the reversible structural evolution of NG particles during charging and discharging (**Fig. 1**). They found C–Cl binding on the surface or edges of NG. Such binding might be a side reaction of the AIB and be partly responsible for the non-ideal Coulombic efficiency (CE) of the cell, and the side reaction that occurs more readily on the edges or surface defects of NG.

An understanding of the variation of the local electronic state of the battery materials in the charging (or oxidation) process was also reported<sup>2</sup> by Yutaka Moritomo (University of Tsukuba) and Di-Jing Huang (NSRRC). Employing resonant inelastic X-ray scattering (RIXS) at **TLS 05A1**, these authors investigated how the local electronic state around the Co site alters in the charging process (**Fig. 2**). They found that that local electronic state around  $\text{Co}^{2+}$  is invariant, within the energy resolution, against partial oxidation. In addition, the local electronic state around the oxidized  $\text{Co}^{3+}$  is essentially the same as that of the fully charged film. Such a strong localization of the oxidized  $\text{Co}^{3+}$  state is advantageous for the reversibility of the redox process, as the localization decreases extra reaction within the materials and resultant deterioration.

In summary, the rate capability in a battery can be significantly improved on constructing a highly porous three-dimensional NG that allows rapid ion diffusion or intercalation. Furthermore, it has also been clarified how far the effect of the

oxidized site spreads and the nature of the electronic state of the oxidized site. The ability to probe electronic structures of electrode materials during charging and discharging makes synchrotron-based soft X-ray spectra and scattering important techniques that provide valuable insight for issues related to batteries. (Reported by Yan-Gu Lin)

*This report features the work of: (1) Bing-Joe Hwang and his co-workers published in Nat. Commun. 8, 14283 (2017); (2) Yutaka Moritomo and his co-workers published in Sci. Rep. 7, 16579 (2017).*

**TLS 20A1 BM – (H-SGM) XAS**  
**TLS 05A1 EPU – Soft X-ray Scattering**

- XANES, RIXS
- Material Science, Chemistry, Condensed Matter Physics

**References**

1. D.-Y. Wang, C.-Y. Wei, M.-C. Lin, C.-J. Pan, H.-L.

Chou, H.-A. Chen, M. Gong, Y. Wu, C. Yuan, M. Angell, Y.-J. Hsieh, Y.-H. Chen, C.-Y. Wen, C.-W. Chen, B.-J. Hwang, C.-C. Chen, and H. Dai, *Nat. Commun.* **8**, 14283 (2017).

2. H. Niwa, M. Takachi, J. Okamoto, W.-B. Wu, Y.-Y. Chu, A. Singh, D.-J. Huang, and Y. Moritomo, *Sci. Rep.* **7**, 16579 (2017).

## Fluoride Phosphors Illuminate a White LED

*A fluoride phosphor that forms a zero-phonon line and exhibits high quantum efficiency was applied successfully in diodes emitting white light.*

To enhance the color-rendering index (CRI) of a device, red-light phosphors are necessary to enrich the red region of the spectrum. As the human eye is least sensitive to red light within the visible region, we barely detect light emitted above wavelength 650 nm. As a result, the broadened band-emission maximum at approximately 650 nm might cause a loss of high energy in the usage of diodes emitting white light (WLED). A fluoride phosphor with high intensity and a line spectrum, with maximum at 630 nm, can be detected by a human eye. Fluoride phosphors show no excitation at 550 nm, which can assist WLED devices to avoid re-absorption, thus making a fluoride phosphor a suitable candidate for use in WLED devices. At present, fluoride phosphors are synthesized with varied chemical compositions. To modify the spectra from fluoride phosphors, a distortion of the crystal is necessary, to cause the formation of the zero-phonon line that gains another line with maximum about 620 nm.

In the study<sup>1</sup> done by Ru-Shi Liu (National Taiwan University) and his co-workers, a new fluoride phosphor, namely,  $\text{Rb}_2\text{GeF}_6:\text{Mn}^{4+}$  (RbGF), was synthesized with the formation of a zero-phonon line (ZPL), which can further improve the color-rendering index of WLED devices. The fabricated RbGF phosphor was applied in a LED, and the performance was compared with the commercial phosphor. The authors applied synchrotron-based X-ray diffraction (XRD) techniques at **TPS 09A** to clarify the detailed structural information of the RbGF samples.

The XRD pattern of RbGF, in which all diffraction signals can be indexed to hexagonal RbGF, indicates that pure single-phase RbGF can be obtained in a hexagonal system with particle size about 30–50

$\mu\text{m}$ . The authors performed a Rietveld refinement to obtain further information about RbGF (**Fig. 1(a)**); this refinement indicates that  $R_p = 2.55\%$  and  $R_{\text{wp}} = 4.80\%$  adequately represent real data, with crystal parameters  $a = 5.958715(8) \text{ \AA}$  and  $c = 9.67058(2) \text{ \AA}$  belonging to the hexagonal system with space group  $P6_3mc$ . The geometry of the  $\text{GeF}_6^{2-}$  site has been simulated (**Fig. 1(b)**); the results of the fit show that the F–Ge–F bond angle is slightly distorted by the

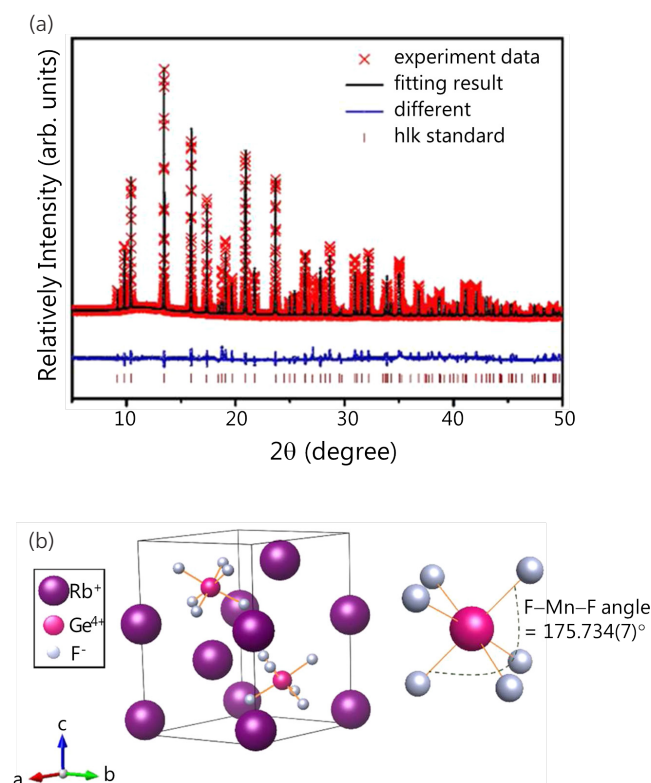


**Fig. 1:** (a) XRD refinement results of  $\text{Rb}_2\text{GeF}_6:\text{Mn}^{4+}$  as prepared, with one pure-phase fit. (b) Simulated refinement model of the  $\text{GeF}_6^{2-}$  site into which activator  $\text{Mn}^{4+}$  was doped. [Reproduced from Ref. 1]